

Geospatial Analysis of the Relationship Between Land Surface Temperature and Land Use/Land Cover indices: A Study of Raiganj Municipality, West Bengal, India

Bapi Sarkar*, Sribas Patra** and, Mallikarjun Mishra***†

*Department of Geography, Raiganj University, Raiganj-733134, West Bengal, India

ORCID: 0000-0003-1871-5250

**Department Geography, Ravenshaw University, Cuttack-753003, Odisha, India

ORCID: 0000-0001-7289-4080

***Department of Geography, Ravenshaw University, Cuttack-753003, Odisha, India

ORCID: 0000-0002-8601-255X

†Corresponding Author: Mallikarjun Mishra; mallikarjungeog@ravenshawuniversity.ac.in

ABSTRACT

The present study is focused on estimation of Land Surface Temperature (LST) and its relationship with three Land Use and Land Cover (LULC) indices--Normalised Difference Vegetation Index (NDVI), Normalised Difference Water Index (NDWI), and Normalised Difference Built-up Index (NDBI) in Raiganj Municipality, India. Landsat-5 TM (2001 & 2011) and Landsat-8 OLI (2021) satellite images were used, processed and analysed in the ArcGIS. The study observed that the values of LST and NDBI were increased by +0.9°C and +0.71 and the values of NDVI and NDWI were decreased by -0.20 and -0.34 during 2001-2021. Highest LST is observed over the built-up spaces and lowest over vegetation cover and water bodies. Result indicates LST has a significant positive correlation with NDBI and negative correlation with NDVI and NDWI. LST is increased due to dramatic changes in LULC specially in unplanned infrastural developmmet and losses in green and blue spaces.

Key Words	Geospatial Techniques; Land Surface Temperature (LST); LU/LC indices, Raiganj
DOI	https://doi.org/10.46488/NEPT.2025.v24i02.B4245 (DOI will be active only after the final publication of the paper)
Citation of the Paper	Bapi Sarkar, Sribas Patra and, Mallikarjun Mishra, 2025. Geospatial analysis of the relationship between land surface temperature and land use/land cover indices: a study of Raiganj municipality, West Bengal, India. <i>Nature Environment and Pollution Technology</i> , 24(2), B4245. https://doi.org/10.46488/NEPT.2025.v24i02.B4245

INTRODUCTION

Land Use/ Land Cover in the urban spaces are rapidly changing, which creates many environmental issues (Herold et al., 2016; Lambin et al., 2003). In a mixed and complex urban environment, the concept of Land Surface Temperature (LST) is utilised to interpret the changing pattern of land use/land cover (LULC) (Guha et al., 2020a; Pal and Ziaul, 2017; Saha et al., 2021). The study of the intensity of LST in major global cities like Beijing, Columbia, Shanghai, Chicago, Mumbai, New Delhi used to address a variety of environmental issues (Asgarian et al., 2015; Das and Das, 2020; Kuang et al., 2014; Mukherjee and Singh, 2020;

O'Connor, 2003; Peng et al., 2020). The nature and distribution of LST are influenced by various LULC indices (Bindajam et al., 2020; Bokaie et al., 2016; Guha and Govil, 2020; Hua and Ping, 2018; Kafy et al., 2020). Vegetation index, built-up index, bareness index, water index, and other normalised difference LULC indices were frequently utilised in recent LST-related studies to quantify their impact on the changing environmental status of urban areas (Aboelnour et al., 2018; Gantumur et al., 2017; Weng, 2009). The relationship between LST and LULC indices using statistical techniques has been explored by the scholars for the different cities (Ferreira and Duarte, 2019, Mallick et al., 2012; Naserikia et al., 2019; Rasul and Ibrahim, 2017; Sekertekin et al., 2015). The linear correlation analysis between the LST and LULC indices were discussed in context of big global cities but very limited to small cities like Raiganj. Li & Zhou, 2019 assessed the seasonal impact of thermal conditions of Ohio city using simple regression analysis and Guha et al., 2020b also assessed seasonal impact of LST on LULC indices in Jaipur city of Rajasthan. Seoul of South Korea (Kim et al., 2022), Anatolian region of Turkey (Karakus, 2019), Dhaka of Bangladesh (Kafy et al., 2021), Yangon city of Myanmar (Yee et al., 2016), Bucharest of Romania (Grigoraş & Urişescu, 2019) are the some examples where relationship between LST and LULC indices has been studied using different model to depict the seasonal fluctuation (Hassan et al., 2021). Major Indian cities are not an exception they are also affected by the ongoing phenomenon of large-scale land-use changes, as a result of globalisation (Chadchan and Shankar, 2012). LST of Indian cities like Bengaluru (Govind & Ramesh, 2020), Chennai (Kaaviya & Devadas, 2021), Delhi (Kant et al., 2009), and Jaipur City (Guha et al., 2020) is continuously increasing due to highly concretization, urbanization, industrialization, transportation, losses in green spaces, changes in local climate, and the establishment of urban heat islands (UHI). Changes in demographic structure creates pressure on the physical environment and its resources (Alberti, 2016; Mersal, 2016; Smyth and Royle, 2000). At a local level a study on English Bazar Municipality of Malda District, West Bengal by Pal & Ziaul (2017) shows seasonal and temporal LST is increased from 0.070⁰ C/year to 0.114⁰ C/year during 1991-2014. Hoque & Lepcha (2019) study on Siliguri Jalpaiguri Development Region shows LST increased 0.34 °C/year from 1991 to 2017, and Sultana & Satyanarayana, 2019 noticed that LST of Kolkata Municipal Corporation (KMC) increased from 10.5°C (2002) to 11.7°C (2013). The present study assessed the relationship between land surface temperature and different LULC indices and evaluates its impact on urban environment of the Raiganj Municipality. Three major LULC Indices--Normalised Difference Vegetation Index (NDVI), Normalised Difference Built-up Index (NDBI), and Normalised Difference Water Index (NDWI) were used in this study to investigate the statistical relationships between these land use indices and LST. The study can be helpful in land use planning by bridging the knowledge gap between present and past conditions and mitigating environmental concerns.

Study Area:

The Raiganj municipality is situated in the south western part of the Uttar Dinajpur district in West Bengal, India. The city received municipal status on August 15, 1951, and it is also popularly known for the Raiganj wildlife sanctuary (popularly known as Kulik bird sanctuary). Geographically, it is situated between 25°34'57''N and 25°38'27''N and latitude, and

88°6'24''E and 88°9'6''E longitude, located 30 meters above sea level. (Fig. 1). The area of the municipality is 10.75 sq. km. and located 425 kilometres away from Kolkata, the state capital of West Bengal. The city of Raiganj is split into 27 wards. With the massive economic expansion and urban agglomeration, the city is designated the district headquarters of Uttar Dinajpur.

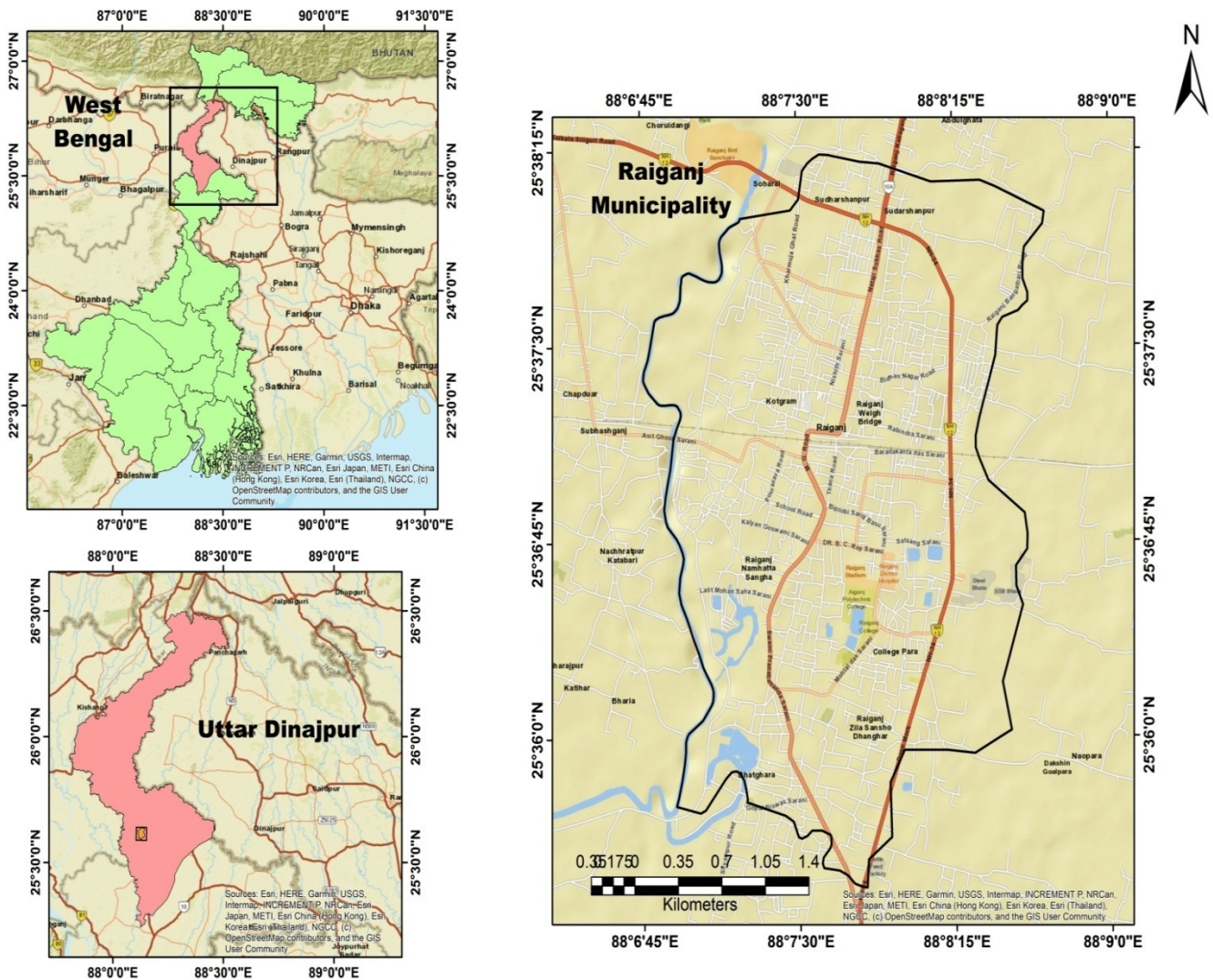


Fig.1: Location map of the study area

MATERIALS AND METHODS

Remote Sensing Data:

Landsat images are updated and available regularly to assist in large-scale landscape studies efficiently. This study uses cloud free multi-temporal Landsat-5 TM (Thematic Mapper) data of 2001 and 2011, as well as Landsat-8 OLI/TIRS (Operational Land Imager/ Thermal Infra-Red Sensor) data of 2021 (Table 1). The data are obtained from United States Geological Survey Earth Explorer Portal (<https://earthexplorer.usgs.gov>).

Table 1: Characteristics of Landsat satellite images used in the present study.

Dataset	Sensor	Year	Acquisition date	Resolution	Path/row	Projections/Datums
Landsat 5	TM	2001	04-02-2001	30m (Band-6, 60 m)	139/42	UTM-WGS1984
Landsat 5	TM	2011	31-01-2011	30m (Band-6, 60 m)	139/42	UTM-WGS1984
Landsat 8	OLI_TIRS	2021	11-02-2021	30m (Band-10-11, 100 m)	139/42	UTM-WGS1984

(Source: USGS Earth Explorer)

Satellite Image Processing:

ERDAS Imagine 14, and Arc GIS 10.3 were used to calculate, analyse and prepare various thematic maps of LST, NDVI, NDBI, and NDWI, derived from satellite images. Calculation of spectral indices and assessment of relationship between LST and other land use indices are the two stages of the present study. The methodological procedure for the study has been summarised in the flowchart (Fig. 2).

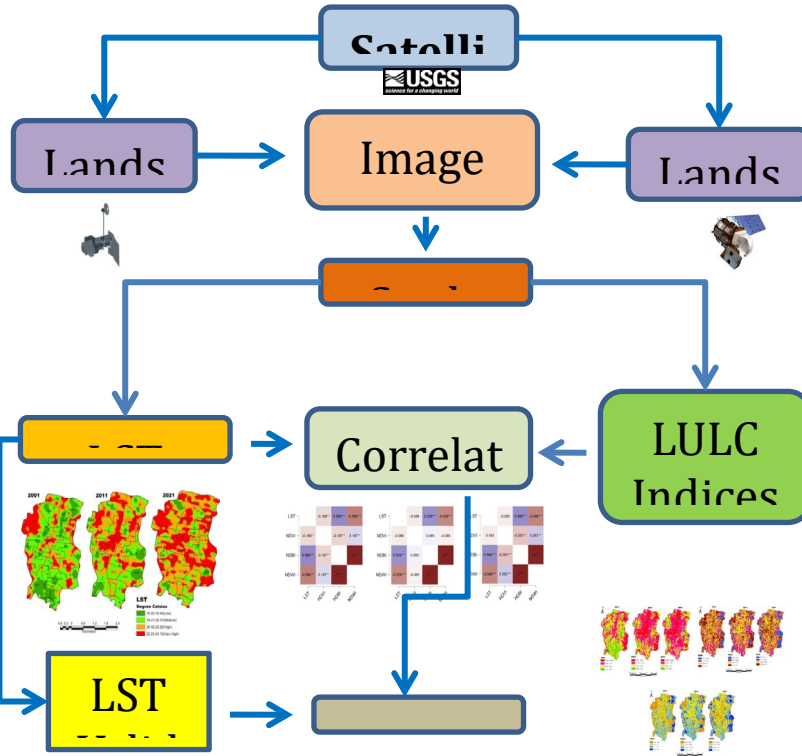


Fig.2:
used in this

Details of the methodology study.

The Derivation of Land Surface Temperature (LST):

Landsat-5 TM of 2001, 2011 and Landsat-8 OLI of 2021 with 0% cloud cover were used to calculate the land surface temperature (LST). Landsat-5 TM provides 7 bands data in which band-6 is a thermal bands, while Landsat-8 OLI imagery provides 11 bands data, in which bands-10 and 11 are thermal bands. The following steps were used for calculation of LST.

Step 1: Conversion of Landsat-5 TM Band-6 digital values to spectral radiances.

The following formula was used to convert band 6 digital values into radiance values ($L\lambda$) (Landsat Project Science Office, 2002)

$$L\lambda = \frac{LMAX\lambda - LMIN\lambda}{QCALMAX - QCALMIN} \times (QCAL - QCALMIN) + LMIN\lambda \quad (1)$$

Here, $L\lambda$ is the atmospherically corrected cell value as the radiance, $QCAL$ is the digital image value, $LMIN\lambda$ is the spectral radiance scaled to $QCALMIN$, $LMAX\lambda$ is the spectral radiance scaled to $QCALMAX$, and $QCALMIN$ is the minimum quantisation calibration. The radiance pixel value (usually 1) and $QCALMAX$ are the maximum values of quantised calibrated pixels (usually 255).

The following formula was used to convert the Landsat-8 OLI/TIRS Band-10 digital values to spectral radiances.

$$L\lambda = ML \times QCAL + AL \quad (2)$$

Where $L\lambda$ is the spectral radiance at the top of the atmosphere, ML denotes the radiance multi-band X, AL denotes the radiance add band X, $QCAL$ denotes the quantised and calibrated

standard product pixel value, and X denotes the band number. The band-specific multiplicative rescaling factor ML and the band-specific additive rescaling factor AL are obtained from the metadata file (MTL file).

Step 2: Satellite brightness spectral radiance temperature conversion and emissivity modification were added to radiant temperature based on the land cover nature following.

$$T = \frac{K_2}{\ln\left(\frac{K_1}{L\lambda} + 1\right)} - 273 \cdot 15 \quad (3)$$

Where T is the satellite brightness temperature in Kelvin (K), $L\lambda$ is the satellite radiance in $W/(m^2sr\mu m)$, and the thermal calibration constants in $W/(m^2sr\mu m)$, respectively. The values of $K_1 = 607.76$, $K_2 = 1260.56$ for band 6 in Landsat-5 TM, and $K_1 = 774.8853$, and $K_2 = 1321.0789$ in Landsat-8 OLI for bands 10 used in the present study taken from (metadata file). For better understanding, the thermal constant values for Landsat TM and Landsat OLI are converted from Kelvin (K) to degrees Celsius ($^{\circ}C$) using the equation $0^{\circ}C = 273.15K$.

Step 3: Emissions from the ground surface are measured (E)

The temperature values derived above are compared to a black body. As a result, spectral emissivity (E) adjustments are required. These can be done according to the land cover type or by calculating the emissivity values for each pixel from the proportion of vegetation (PV) data.

$$E = 0.004 * PV + 0.986 \quad (4)$$

Where, the proportion of vegetation (PV) can be calculated as:

$$P_V = \left\{ \frac{(NDVI_{max} - NDVI_{min})}{(NDVI_{max} - NDVI_{min})} \right\}^2 \quad (5)$$

Step 4: Calculation of Land Surface Temperature (LST).

LST is calculated using the equation given below.

$$\frac{BT}{1} + W * \left(\frac{BT}{P} \right) * \ln(E) \quad (6)$$

Where BT is the brightness temperature at the satellite image, W is the wavelength of emitted radiance, $P = h \cdot c / s$ ($1.438 \cdot 10^{-2}$ m K), h is the Planck's constant ($6.626 \cdot 10^{-34}$ Js), s is the boltzmann constant ($1.38 \cdot 10^{-23}$ J/K), and c is the velocity of light ($2.998 \cdot 10^8$ m/s).

Retrieval of LULC Indices:

The following method were used to determine the relationship between LST and three spectral indices--NDVI (Normalized Difference Vegetation Index), NDWI (Normalized Difference Water Index), and NDBI (Normalized Difference Built-Up Index) (Equations 7 to 9).

Calculation of Normalized Difference Vegetation Index (NDVI)

The NDVI values was extracted using the approach given by Cityshend and Justice (1986)

$$NDVI = \frac{(NIR \text{ band} - R \text{ band})}{(NIR \text{ band} + R \text{ band})} \quad (7)$$

Where *NIR* is the Near-InfraRed band's DN (digital number) value (Band-4 for landsat 5 and band-5 for landsat 8) and *R* is the red band's *DN* value (Band-3 for landsat 5 and band-4 for landsat 8). The NDVI value is a number that ranges between -1 to +1. Low vegetation cover is indicated by values close to 0, and high vegetation density is indicated by values close to 1.

Calculation of Normalized Difference Water Index (NDWI)

$$NDWI = \frac{(Greenband - NIRband)}{(Green\ band - NIR\ band)} \quad (8)$$

To avoid the problem of the built-up area being included in the *NIR* band (Band-4 for landsat 5 and Band-5 for landsat 8) NDWI is used, where green refers to the green band (Band-2 landsat for 5 and Band-3 for landsat 8), and *NIR* refers to the near-infrared band.

Calculation of Normalized Difference Built-up Index (NDBI)

Formula used by Zha et al. (2003) is used to calculate NDBI with a value closer to 1 indicating a high density of built-up land.

$$NDBI = \frac{(MIR\ band - NIR\ band)}{(MIR\ band + NIR\ band)} \quad (9)$$

Where *MIR* (Band-5 for Landsat-5 and Band-6 for Landsat-8) is the DN from the Mid-InfraRed band and *NIR* (Band-4 for landsat 5 and band-5 for landsat 8) is the Near-InfraRed band.

Following formula of Pearson's product-moment correlation coefficient (*r*) is used in the present study. is used in (Patra and Gavsker, 2021)

$$r = \frac{n(\sum xy) - (\sum x)(\sum y)}{\sqrt{[n\sum x^2 - (\sum x)^2][n\sum y^2 - (\sum y)^2]}} \quad (10)$$

$$y_i = \beta_0 + \beta^1 x_i^1 + \beta^2 x_i^2 + \dots + \beta_p x_{ip} + \epsilon \quad (11)$$

where, for *i* = *n* observations,

y_i = dependent variable,

x_i = explanatory variables,

β_0 = y-intercept (constant term),

β_p = slope coefficients for each explanatory variable,

ϵ = the model's error term (also known as the

Maps derived from the calculation of spectral indices-NDVI, NDWI and NDBI shows geographical distribution of vegetation cover, water coverage, and built-up areas of the municipality during the study period.

RESULT AND DISCUSSION

Spatio-temporal distribution of Land Surface Temperature (LST):

Land surface temperature (LST) of Raiganj Municipality has been derived to know how the LST distribution has changed over a period of time (Table 2 & Fig. 3). The result shows that value of the LST increases throughout the study period. LST in 2001 with low radiant temperature ranges between 16.50-18.40 °C covers an area of 2.02 sq. km. (17.77% of the total study area) distributed over wards--1,3,10, 25, 26, and 27. And, very high radiant temperature ranges between 22.23°C-24.13°C covers an area of 1.96 sq. km. (17.31% of the total area) distributed over wards--7, 9, 13, 20, and 21. Medium to high temperature ranges between 18.41°C-22.22°C covers rest of the wards accounts 7.37 sq.km. area (64.92% of the total area).

LST in 2011 with low radiant temperature ranges between 16.50 °C -18.40 °C covers an area of 1.88 sq.km. (16.56% whole area) distributed over wards--13,20, and 27. The very high radiant temperature ranges between 22.23 °C -24.13 °C covers an area of 2.02 sq.km. (17.80 % of total area) distributed over wards--2, 5, 7, 10, 13, 14, 15, and 21 (Fig. 3). Medium to high temperature observed mainly parts of ward no 2-3, 5, and 9. The low radiant temperature ranges between 16.50°C-18.40°C covers an area of 1.05 sq.km which distributed over wards--6, 20 and 27 in 2021. Very high radiant temperature ranges between 22.23°C-24.13°C covers an area of 2.46 sq.km. (21.67 % of the study area) mainly distributed over wards-7-9,13,14,15, 20, 21 and, 22 (Table 3). The result indicates that, LST has changed over time in different land-use units, particularly in north-western portion, noticed high range of temperature prevailed from 2001 to 2021. LST has increased significantly over each land cover unit, particularly over built-up spaces, sand deposited areas, and water bodies. For the validation of Landsat-derived LST, Terra MODI11A2 products were used. The MODI11A2 product is available from 2001 to 2021. The Root Mean Square Error (RMSE) value acquired was 0.81°C and the r (Pearson correlation coefficient) value was seen as 0.94. the result shows the LST value acquired from Landsat imageries is highly reliable for this study area. According to the correlation value, LST values for MODIS and Landsat are highly correlated.

Table 2: Statistical description of Land Surface Temperature of years--2001, 2011, and 2021

Year	2001	2011	2021
Maximum	22.821	21.066	23.717
Minimum	17.023	16.565	19.382
Mean	19.465	18.527	21.680
SD	0.967	0.544	0.548

Table 3: Decadal descriptive statistics of Land Surface Temperature

Category	Temperature (°C)	Years					
		2001		2011		2021	
		Area(sq.km.)	Percentage	Area(sq.km.)	Percentage	Area(sq.km.)	Percentage
Low	16.50-18.40	2.02	17.77	1.88	16.56	1.05	9.24

Medium	18.41-20.31	4.77	41.99	4.71	41.53	3.60	31.73
High	20.32-22.22	2.60	22.93	2.74	24.11	4.24	37.35
Very High	22.23-24.13	1.96	17.31	2.02	17.80	2.46	21.67
Total		11.35	100	11.35	100	11.35	100

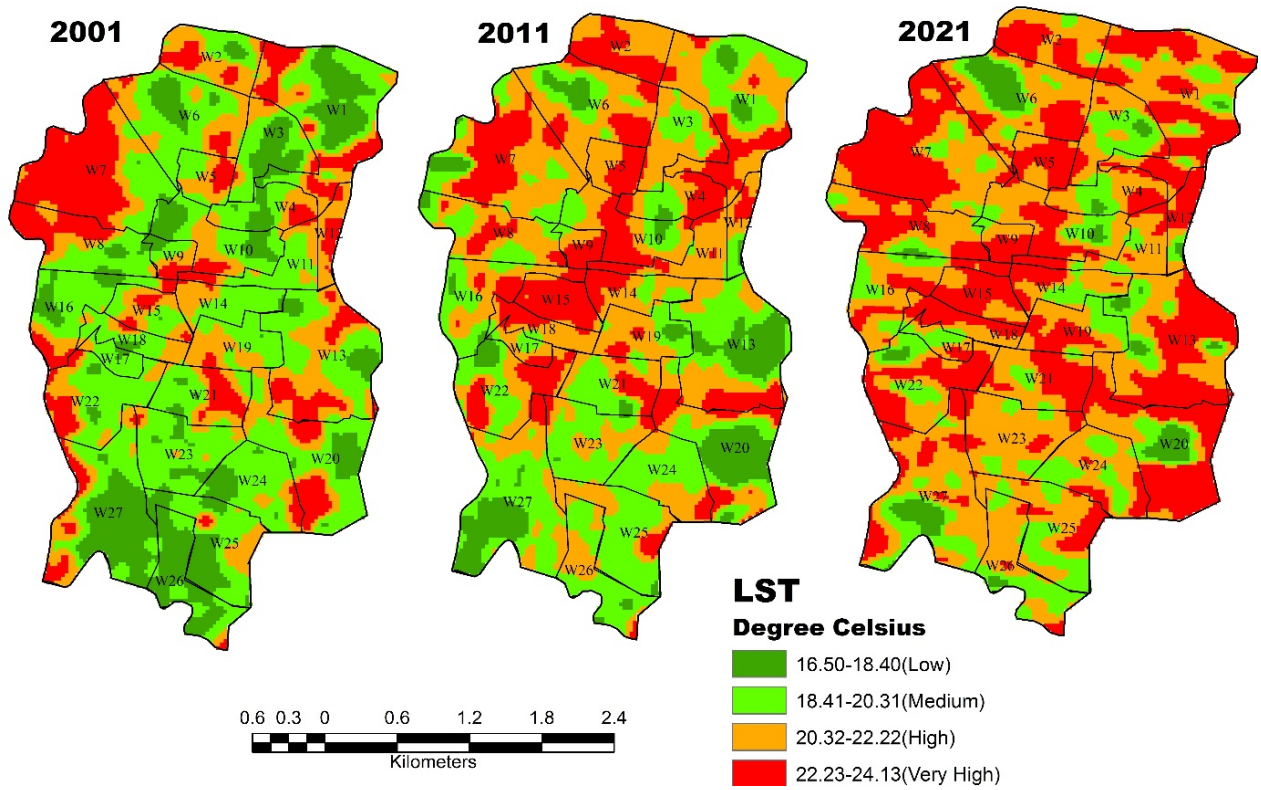
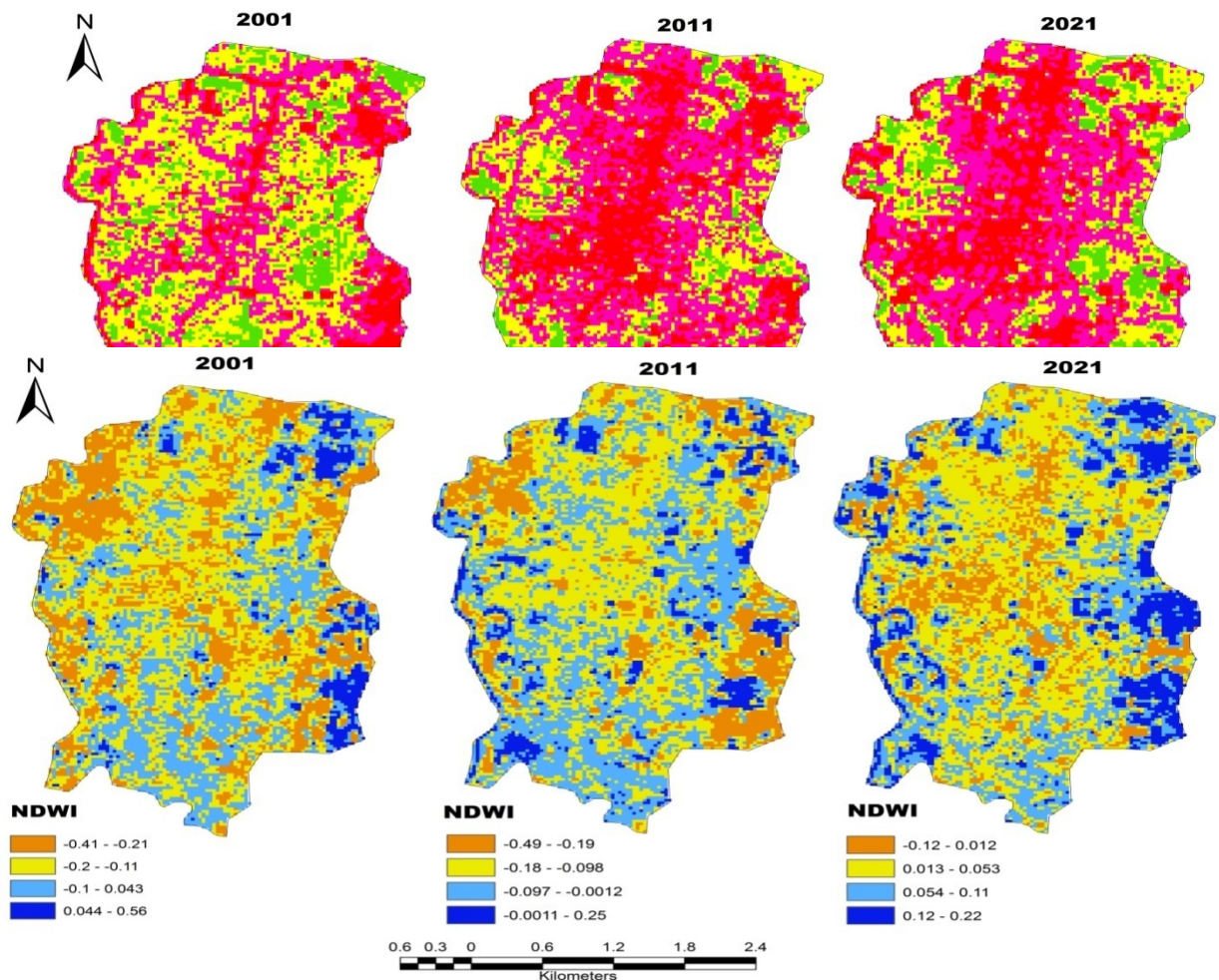


Fig.3: Spatial distribution of LST of 2001, 2011, and 2021.

Analysis of Spatial Characteristics of NDVI, NDBI, and NDWI:

NDVI, NDBI, and NDWI were used to create maps and statistical analysis over different periods (2001, 2011, and 2021). Decadal descriptive statistics of NDVI, NDWI, and NDBI are given in the Table 2. For the years 2001, 2011, and 2021, NDVI was used to determine the vegetation condition of the study area (Fig. 4). NDVI maps extracted from the Landsat images of years--2001, 2011 and 2021 shows in impervious surface, there is a notable decrease of vegetation cover (scattered vegetation and woodland). The area covered with waterbodies also shows low NDVI values. The highest value of the NDVI in 2001 is 0.466 and in 2021 is 0.264 which means there is a decreasing trend in vegetation cover and loss in conditions and increasing of trend in impervious surface (builtup spaces). (Table 3).

Fig.4: Spatial distribution of NDVI of 2001, 2011 and 2021.



NDWI maps of years-2001, 2011, and 2021 shows the NDWI pattern (Fig. 5). There is a significant change in the coverage of the water bodies, as the maximum NDWI value was decreased from 0.56 (2001) to 0.22 (2021). The highest NDWI value belongs to water body, and the lowest NDWI concentration is indicating the impervious surface (buildings, roads, bridges etc.). At some extent, the presence of water bodies aids in lowering its own and the surrounding areas temperature (Table 4).

Fig.5: Spatial distribution of NDWI of 2001, 2011 and 2021.

Built-up maps are created by visualising the area's built-up growth using the NDBI (Normalised Difference Built-up Index) (Fig. 6). Built-up and densely populated areas have high NDBI values. Due to land use conversion in industrial and commercial buildings, residential buildings, roads, and transportation communication from other land use features (Green and Blue Cover). Maximum NDBI value significantly increased over these land use areas. As a result, high NDBI values can be seen in built-up areas and other impervious surfaces, whereas low NDBI values can be seen over water bodies and vegetation cover (Table 4).

Table 4: The Statistical Description of NDVI, NDWI, and NDBI in study years.

LULC indices	YEAR	2001	2011	2021
NDVI	Minimum	-0.31	-0.123	-0.027
	Maximum	0.466	0.171	0.264
	Mean	0.146	0.005	0.089
	SD	0.087	0.033	0.035
NDWI	Minimum	-0.405	-0.494	-0.117
	Maximum	0.565	0.25	0.224
	Mean	-0.137	-0.109	0.050
	SD	0.110	0.083	0.046
NDBI	Minimum	-0.565	-0.25	-0.224
	Maximum	0.405	0.494	1.117
	Mean	0.137	0.109	-0.050
	SD	0.110	0.083	0.046

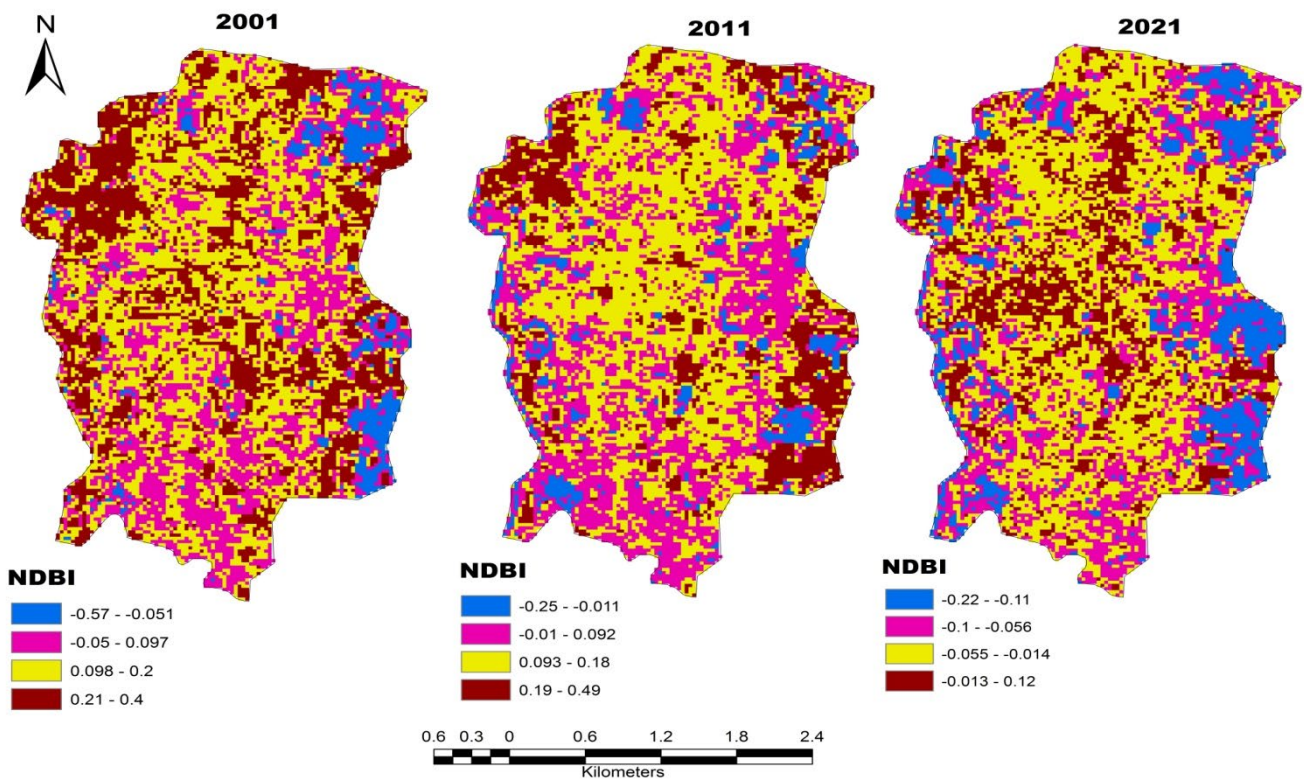


Fig.6: Spatial distribution of NDBI of 2001, 2011 and 2021.

Correlation and regression between LST and LULC Indices:

In 2001, the significant negative relation was observed mainly between LST and all three LULC indices--NDWI, NDBI, NDVI (Fig.7). In 2021, it was shown that there was a significant negative relationship between LST and NDVI and positive relationship between LST and NDBI (Fig.7). Result indicates that temperature increases over built-up land and gradually decreases over vegetation cover. Here also retrieved values of the selected parameters (LST, NDVI, NDWI, and NDBI) were used to build a regression model. The association between LST and various LULC indices of LULC was studied using a linear regression model for each land use types separately. The area, where the R^2 (coefficient of determination) produced from the regression model is 0.394, 0.401, and 0.608 for 2001, 2011, and 2021 years shows there is a strong negative connection (Fig. 8) between land surface temperature (LST) and vegetation cover. The high R^2 value in 2021 shows that vegetation cover is significantly reduces and surface radiative temperature is gradually increased (Fig. 8).

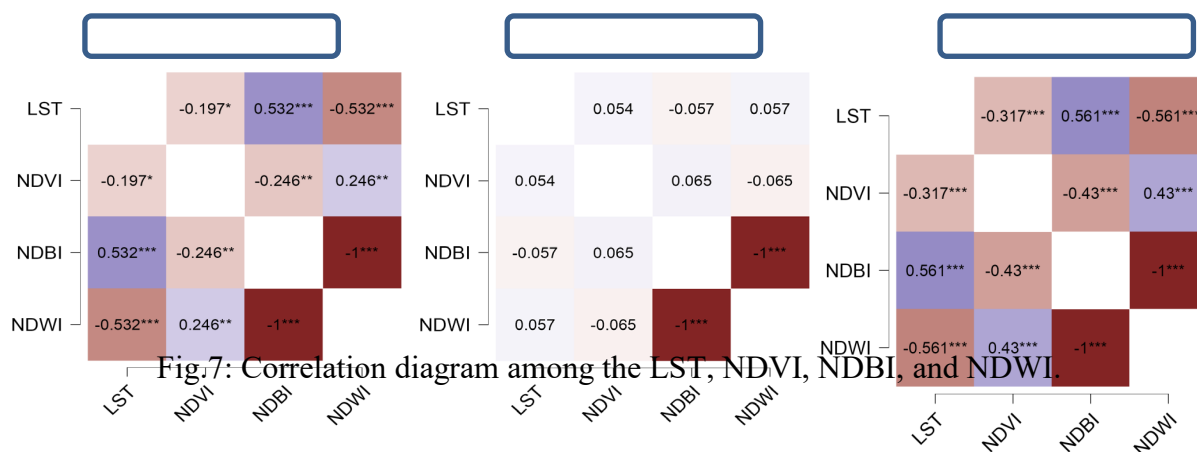


Fig.7: Correlation diagram among the LST, NDVI, NDBI, and NDWI.

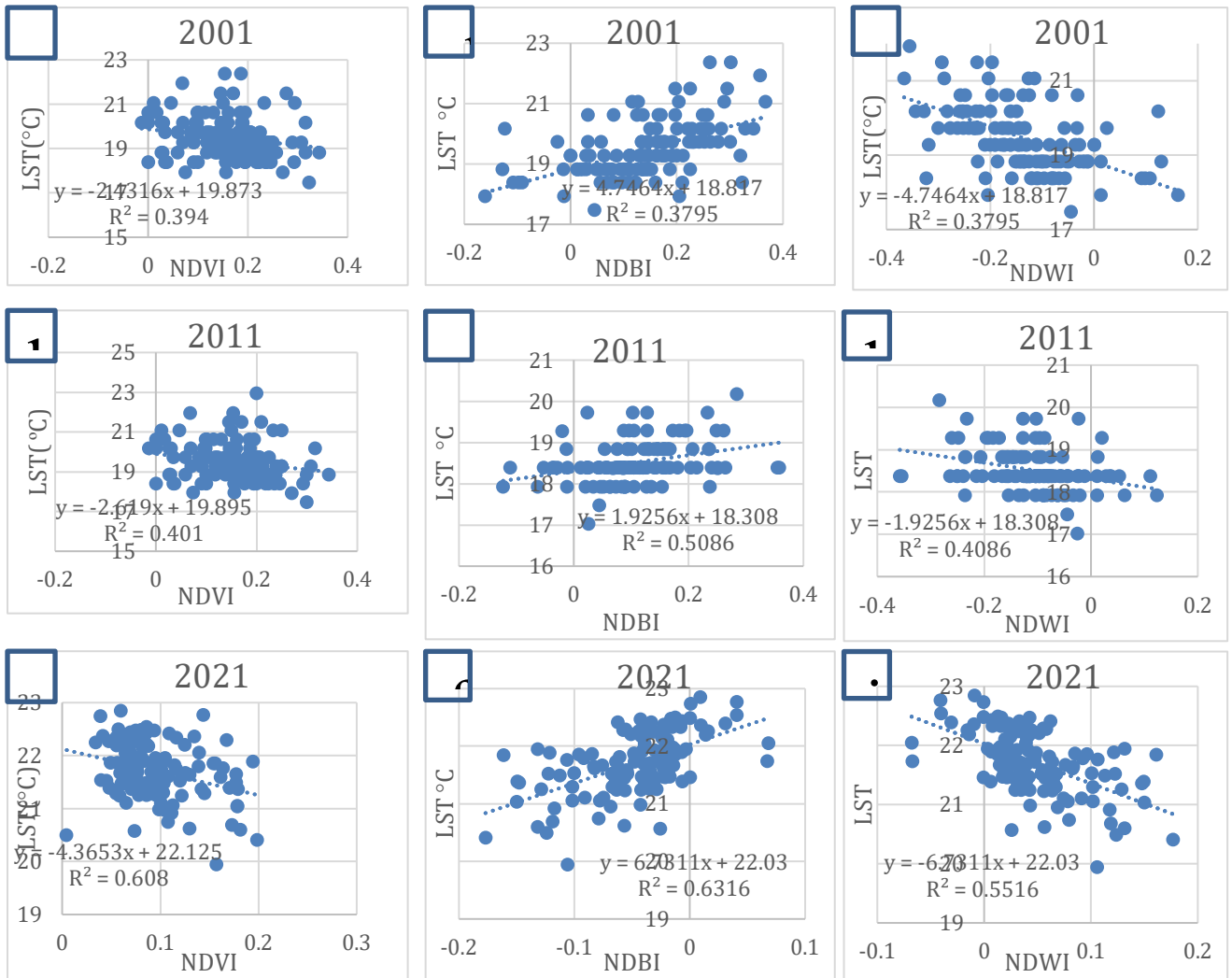


Fig.8: Correlation between LST and NDVI (a, b, and c); LST and NDBI (d, e, and f); LST and NDWI (g, h, and i)

LST and NDWI have a negative connection, signifying lower temperatures over water bodies and higher temperatures in non-water body areas. The linear regression model reveals association with an R² of 0.379, 0.4086, and 0.551 in the years--2001, 2011, and 2021, respectively (Fig. 8). The higher R² value in 2021 (Fig. 8) shows that water bodies play an important role in reducing surface radiative temperature (Fig. 5). The perfect positive relationship between LST and NDBI can be seen in Fig. 8. In 2021, the R² value generated by the model was 0.6316, which is higher than in 2001. The fact that a rise in built-up or impermeable surfaces captured the radiation that positively controls LST was established by such a high value of R² (Fig. 8). As a result, the land surface temperature (LST) is sensitive to each form of land use; it can be used to detect changes in land use and land cover.

CONCLUSION

Landsat-5 TM and Landsat-8 OLI of different years have been used to investigate the dynamic relationship between LST with NDVI, NDWI, and NDBI and evaluate the environmental

impact of urbanisation in terms of reduced green space and increased land surface temperature, UHI intensity effect in the area. At the pixel level, the associations between LST and NDVI, NDWI, and NDBI have been quantified using linear regression analysis. Conclusions drawn from the present study are given below--

1. The land use pattern in Raiganj city is changing at faster rate. Vegetation cover and agricultural land have been occupied, and open spaces and wetlands have been converted into infrasturral areas.
2. The study found that changing LULC significantly influences on land surface temperature.
3. LST has a significant positive association with NDBI and a moderate to strong negative correlation with NDVI and NDWI.
4. The study shows that the radiative surface temperature is regulated by green space, and the distribution of the UHI is significantly influenced by plant cover in the urban area.
5. UHIs have been identified through the spatial distribution of LST, which mainly existed in bare land and built-up areas; this area is primarily responsible for accumulating high LST values in the city. LST level is reduced significantly due to the presence of vegetation cover and water bodies.

The researcher, policy-maker, and administrators of Raiganj city can benefit from present study for urban planning and management. This study has its own limitations, First, LST can be derived by using other high-resolution satellite datasets--IKONOS (1m), Quickbird (0.6m), ASTER (15m), Sentinel-2A (10m) to carry out the complete research, second, the in-situ measurement or validation of the satellite derived LST with temperature data collected from the field can give better outcome.

Acknowledgement: Author's are thankful to the reviewers for giving critical comments to improve the quality of the manuscript.

Author Contribution: B.S., S.P., and M.M. jointly designed the experiments. B.S. and S.P. carried out the experiment and analysis was done by B.S., S.P. and M.M.. Manuscript was written by B.S., S.P. and M.M.. S.P., and M.M. prepared the final draft of the manuscript.

Funding: No funding was received by author's.

Conflict of Interest: Authors declares no conflict of interest.

Data Availability: The datasets generated during and/or analysed during the current study are available from the corresponding author on reasonable request.

REFERENCES

- Aboelnour M., Engel B.A., Aboelnour M. and Engel B.A. 2018. Application of Remote Sensing Techniques and Geographic Information Systems to Analyze Land Surface Temperature in Response to Land Use/Land Cover Change in Greater Cairo Region, Egypt. *Journal of Geographic Information System*, 10(1), 57–88. DOI: 10.4236/JGIS.2018.101003
- Alberti M. 2016. Modeling the Urban Ecosystem: A Conceptual Framework: <https://doi.org/10.1068/B260605>, 26(4), 605–630. DOI: 10.1068/B260605

- Asgarian A., Amiri B.J. and Sakieh Y. 2015. Assessing the effect of green cover spatial patterns on urban land surface temperature using landscape metrics approach. *Urban Ecosystems*, 18(1), 209–222. DOI: 10.1007/S11252-014-0387-7
- Bindajam A.A., Mallick J., AlQadhi S., Singh C.K. and Hang H.T. 2020. Impacts of vegetation and topography on land surface temperature variability over the semi-arid mountain cities of Saudi Arabia. *Atmosphere*, 11(7), 1–28. DOI: 10.3390/ATMOS11070762
- Bokaie M., Zarkesh M.K., Arasteh P.D. and Hosseini A. 2016. Assessment of Urban Heat Island based on the relationship between land surface temperature and Land Use/ Land Cover in Tehran. *Sustainable Cities and Society*, 23, 94–104. DOI: 10.1016/j.scs.2016.03.009
- Chadchan J. and Shankar R. 2012. An analysis of urban growth trends in the post-economic reforms period in India. *International Journal of Sustainable Built Environment*, 1(1), 36–49. DOI: 10.1016/J.IJSBE.2012.05.001
- Chen, L., Li, M., & Huang, F. 2013. *Relationships of LST to NDBI and NDVI in Wuhan City Based on Landsat ETM + Image. Cisp*, 840–845.
- Chen, L., Wang, X., Cai, X., Yang, C., & Lu, X. 2021. *Seasonal Variations of Daytime Land Surface Temperature and Their Underlying Drivers over Wuhan , China*. 1–22.
- Das M. and Das A. 2020. Urban Climate Assessing the relationship between local climatic zones (LCZs) and land surface temperature (LST) – A case study of Sriniketan- Santiniketan Planning Area (SSPA), West Bengal , India. *Urban Climate*, 32(January), 100591. DOI: 10.1016/j.uclim.2020.100591
- Ferreira L.S. and Duarte D.H.S. 2019. Exploring the relationship between urban form, land surface temperature and vegetation indices in a subtropical megacity. *Urban Climate*, 27, 105–123. DOI: 10.1016/J.UCLIM.2018.11.002
- Gantumur B., Wu F., Zhao Y., Vandansambuu B., Dalaibaatar E., Itiritiphan F. and Shaimurat D. 2017. Implication of relationship between natural impacts and land use/land cover (LULC) changes of urban area in Mongolia. <https://doi.org/10.1117/12.2278360>, 10431, 139–157. DOI: 10.1117/12.2278360
- Govind, N. R., & Ramesh, H. 2020. Exploring the relationship between LST and land cover of Bengaluru by concentric ring approach. *Environmental Monitoring and Assessment*, 192(10). <https://doi.org/10.1007/s10661-020-08601-x>
- Grigoraş, G., & Urişescu, B. 2019. Land Use/Land Cover changes dynamics and their effects on Surface Urban Heat Island in Bucharest, Romania. *International Journal of Applied Earth Observation and Geoinformation*, 80(February), 115–126. <https://doi.org/10.1016/j.jag.2019.03.009>
- Guha S. and Govil H. 2020. Seasonal impact on the relationship between land surface temperature and normalized difference vegetation index in an urban landscape. <https://doi.org/10.1080/10106049.2020.1815867>. DOI: 10.1080/10106049.2020.1815867
- Guha, S., Govil, H., Gill, N., & Dey, A. 2020a. Annals of GIS Analytical study on the relationship between land surface temperature and land use / land cover indices. *Annals of GIS*, 26(2), 201–216. <https://doi.org/10.1080/19475683.2020.1754291>
- Guha S., Govil H., Gill N. and Dey A. 2020b. Analytical study on the relationship between land surface temperature and land use/land cover indices. *Annals of GIS*, 26(2), 201–216. DOI: 10.1080/19475683.2020.1754291
- Guha, S., & Govil, H. 2021. A long-term monthly analytical study on the relationship of LST with normalized difference spectral indices. *European Journal of Remote Sensing*, 54(1), 487–511. <https://doi.org/10.1080/22797254.2021.1965496>
- Guha, S., & Govil, H. 2022. Annual assessment on the relationship between land surface temperature and six remote sensing indices using landsat data from 1988 to 2019. *Geocarto International*, 37(15), 4292–4311. <https://doi.org/10.1080/10106049.2021.1886339>
- Hassan T., Zhang J., Prodhan F.A., Pangali Sharma T.P. and Bashir B. 2021. Surface urban heat islands dynamics in response to lulc and vegetation across south asia (2000–2019). *Remote Sensing*, 13(16), 1–24. DOI: 10.3390/rs13163177
- Herold M., Scepan J. and Clarke K.C. 2016. The Use of Remote Sensing and Landscape Metrics to Describe Structures and Changes in Urban Land Uses: <http://dx.doi.org/10.1068/A3496>, 34(8), 1443–1458. DOI: 10.1068/A3496

- Hoque, I., & Lepcha, S. K. 2019. A geospatial analysis of land use dynamics and its impact on land surface temperature in Siliguri Jalpaiguri development region , West Bengal. *Applied Geomatics*, 12(2), 163–178. <https://doi.org/10.1007/s12518-019-00288-1>
- Hua A.K. and Ping O.W. 2018. The influence of land-use/land-cover changes on land surface temperature: a case study of Kuala Lumpur metropolitan city. <https://doi.org/10.1080/22797254.2018.1542976>, 51(1), 1049–1069. DOI: 10.1080/22797254.2018.1542976
- Kaaviya, R., & Devadas, V. 2021. Water resilience mapping of Chennai, India using analytical hierarchy process. *Ecological Processes*, 10(1), 1–22. <https://doi.org/10.1186/s13717-021-00341-1>
- Kafy A. Al, Rahman M.S., Faisal A. Al, Hasan M.M. and Islam M. 2020. Modelling future land use land cover changes and their impacts on land surface temperatures in Rajshahi, Bangladesh. *Remote Sensing Applications: Society and Environment*, 18, 100314. DOI: 10.1016/J.RSASE.2020.100314
- Kafy, A. Al, Dey, N. N., Al Rakib, A., Rahaman, Z. A., Nasher, N. M. R., & Bhatt, A. 2021. Modeling the relationship between land use/land cover and land surface temperature in Dhaka, Bangladesh using CA-ANN algorithm. *Environmental Challenges*, 4(May), 100190. <https://doi.org/10.1016/j.envc.2021.100190>
- Kant, Y., Bharath, B. D., Mallick, J., Atzberger, C., & Kerle, N.2009. Satellite-based analysis of the role of land use/land cover and vegetation density on surface temperature regime of Delhi, india. *Journal of the Indian Society of Remote Sensing*, 37(2), 201–214. <https://doi.org/10.1007/s12524-009-0030-x>
- Karakuş, C. B. 2019. The Impact of Land Use/Land Cover (LULC) Changes on Land Surface Temperature in Sivas City Center and Its Surroundings and Assessment of Urban Heat Island. *Asia-Pacific Journal of Atmospheric Sciences*, 55(4), 669–684. <https://doi.org/10.1007/S13143-019-00109-W>
- Kim, M., Kim, D., & Kim, G. 2022. Examining the Relationship between Land Use/Land Cover (LULC) and Land Surface Temperature (LST) Using Explainable Artificial Intelligence (XAI) Models: A Case Study of Seoul, South Korea. *International Journal of Environmental Research and Public Health*, 19(23). <https://doi.org/10.3390/ijerph192315926>
- Kuang W., Liu Y., Dou Y., Chi W., Chen G., Gao C., Yang T., Liu J. and Zhang R. 2014. What are hot and what are not in an urban landscape: quantifying and explaining the land surface temperature pattern in Beijing, China. *Landscape Ecology* , 2014 30:2, 30(2), 357–373. DOI: 10.1007/S10980-014-0128-6
- Lambin E.F., Geist H.J. and Lepers E. 2003. Dynamics of Land-Use and Land-Cover Change in Tropical Regions. <https://doi.org/10.1146/Annurev.Energy.28.050302.105459>, 28, 205–241. DOI: 10.1146/ANNUREV.ENERGY.28.050302.105459
- Li T., Cao J., Xu M., Wu Q. and Yao L. 2020. The influence of urban spatial pattern on land surface temperature for different functional zones. *Landscape and Ecological Engineering*, 16(3), 249–262. DOI: 10.1007/s11355-020-00417-8
- Mallick J., Singh C.K., Shashtri S., Rahman A. and Mukherjee S.2012. Land surface emissivity retrieval based on moisture index from LANDSAT TM satellite data over heterogeneous surfaces of Delhi city. *International Journal of Applied Earth Observation and Geoinformation*, 19(1), 348–358. DOI: 10.1016/J.JAG.2012.06.002
- Mersal A. 2016. Sustainable Urban Futures: Environmental Planning for Sustainable Urban Development. *Procedia Environmental Sciences*, 34, 49–61. DOI: 10.1016/J.PROENV.2016.04.005
- Mukherjee F. and Singh D. 2020. Assessing Land Use–Land Cover Change and Its Impact on Land Surface Temperature Using LANDSAT Data: A Comparison of Two Urban Areas in India. *Earth Systems and Environment* 2020 4:2, 4(2), 385–407. DOI: 10.1007/S41748-020-00155-9
- Naserikia M., Shamsabadi E.A., Rafieian M. and Filho W.L. 2019. The urban heat island in an urban context: A case study of Mashhad, Iran. *International Journal of Environmental Research and Public Health*, 16(3). DOI: 10.3390/ijerph16030313
- O’Connor K. 2003. Global air travel: Toward concentration or dispersal? *Journal of Transport Geography*, 11(2), 83–92. DOI: 10.1016/S0966-6923(03)00002-4
- Pal S. and Ziaul S. 2017. Detection of land use and land cover change and land surface temperature in English Bazar urban centre. *Egyptian Journal of Remote Sensing and Space Science*, 20(1), 125–145. DOI: 10.1016/j.ejrs.2016.11.003
- Patra S. and Gavsker K.K. 2021. Land use and land cover change-induced landscape dynamics: A geospatial study of Durgapur Sub-Division, West Bengal (India). *Acta Universitatis Carolinae, Geographica*, 56(1), 79–94. DOI: 10.14712/23361980.2021.3

- Peng X., Wu W., Zheng Y., Sun J., Hu T. and Wang P. 2020. Correlation analysis of land surface temperature and topographic elements in Hangzhou, China. *Scientific Reports* 2020 10:1, 10(1), 1–16. DOI: 10.1038/s41598-020-67423-6
- Rasul G. and Ibrahim F. 2017. *Urban Land Use Land Cover Changes and Their Effect on Land Surface Temperature : Case Study Using Dohuk City in the Kurdistan Region of Iraq*. DOI: 10.3390/cli5010013
- Saha S., Saha A., Das M., Saha A., Sarkar R. and Das A. 2021. Analyzing spatial relationship between land use/land cover (LULC) and land surface temperature (LST) of three urban agglomerations (UAs) of Eastern India. *Remote Sensing Applications: Society and Environment*, 22(April), 100507. DOI: 10.1016/j.rsase.2021.100507
- Sekertekin A., Kutoglu S.H. and Kaya S. 2015. Evaluation of spatio-temporal variability in Land Surface Temperature: A case study of Zonguldak, Turkey. *Environmental Monitoring and Assessment* 2015 188:1, 188(1), 1–15. DOI: 10.1007/S10661-015-5032-2
- Smyth C.G. and Royle S.A. 2000. Urban landslide hazards: incidence and causative factors in Niterói, Rio de Janeiro State, Brazil. *Applied Geography*, 20(2), 95–118. DOI: 10.1016/S0143-6228(00)00004-7
- Sultana, S., & Satyanarayana, A. N. V. 2019. Impact of urbanisation on urban heat island intensity during summer and winter over Indian metropolitan cities. *Environmental Monitoring and Assessment*, 191. <https://doi.org/10.1007/s10661-019-7692-9>
- Yee, K. M., Ahn, H., Shin, D., & Choi, C. 2016. Relationship assessment among land use and land cover and land surface temperature over downtown and suburban areas in Yangon City, Myanmar. *Korean Journal of Remote Sensing*, 32(4), 353–364. <https://doi.org/10.7780/kjrs.2016.32.4.2>